J Mater Sci: Mater Electron (2017) 28:17849–17859
DOI 10.1007/s10854-017-7726-4

Schiff-base hydrothermal synthesis and characterization of Nd_2O_3 nanostructures for effective photocatalytic degradation of eriochrome black T dye as water contaminant

Sahar Zinatloo-Ajabshir[1] · Sobhan Mortazavi-Derazkola[2] · Masoud Salavati-Niasari[2]

Received: 26 June 2017 / Accepted: 14 August 2017 / Published online: 21 August 2017

Abstract $Nd(OH)_3$ nanostructures have been prepared through a new simple hydrothermal approach with $Nd(NO_3)_3{\cdot}6H_2O$ and tetraethylenepentamine (tepa) as starting materials in presence of bis-(2-hydroxynaphthaldehyde)-1,2-phenylenediamine as novel capping agent. Bis-(2-hydroxynaphthaldehyde)-1,2-phenylenediamine was employed as capping agent in presence of tepa to produce nanostructured $Nd(OH)_3$ for the first time. Pure hexagonal Nd_2O_3 nanostructures with superior photocatalytic activity were synthesized by thermal conversion of nanostructured $Nd(OH)_3$ in air at 700 °C for 4 h. The formation of as-obtained nanostructures and their structure and shape were analyzed by Fourier transform infrared (FT-IR) spectroscopy, scanning electron microscopy (SEM), UV–vis diffuse reflectance spectroscopy, energy dispersive X-ray microanalysis (EDX), X-ray diffraction (XRD) and transmission electron microscopy (TEM). By varying the precipitator type, reaction time and applying Schiff base ligand as novel capping agent, the approach permits us to produce samples with various particle sizes and shapes. In addition, the photocatalytic performance of as-produced Nd_2O_3 samples with various particle sizes and shapes was investigated by degradation of eriochrome black T dye as water contaminant.

✉ Masoud Salavati-Niasari
salavati@kashanu.ac.ir

[1] Young Researchers and Elites Club, Arak Branch, Islamic Azad University, Arak, Islamic Republic of Iran

[2] Institute of Nano Science and Nano Technology, University of Kashan, P. O. Box. 87317-51167, Kashan, Islamic Republic of Iran

1 Introduction

Research on the synthesis of the nanostructured materials is a noteworthy field in modern scientific and industrial studies [1–7]. One of these nanostructured materials is Nd_2O_3. Nd_2O_3 as a remarkable rare earth metal oxide due to its specific, exceptional and noteworthy optical and electrical characteristics is widely employed in the advanced materials, thin films, photonic, luminescent and thermoluminescent materials, protective coatings and catalysts [8–13].

In recent years, hydrogen plasma-metal reaction, microemulsion, gel combustion, solution-coprecipitation, thermal decomposition and hydrothermal routes [13–19] have been introduced to prepare Nd_2O_3. Control over grain size and shape of the nanostructured materials is a new challenge in the modern scientific and industrial studies [20–23]. Among the different ways developed for the production of the nanostructured materials, hydrothermal procedure has been proven to be a facile and reproducible approach, particularly to control the grain size and shape of the nanostructured materials.

Herein, we developed a new simple morphology-controlled way to synthesize $Nd(OH)_3$ nanostructures applying $Nd(NO_3)_3{\cdot}6H_2O$ and tetraethylenepentamine (tepa) as starting materials in presence of bis-(2-hydroxynaphthaldehyde)-1,2-phenylenediamine as novel capping agent under hydrothermal conditions. In addition, nanostructured Nd_2O_3 nanostructures can be synthesized by calcination of as-obtained nanostructured $Nd(OH)_3$ at 700 °C. To our knowledge, it is the first time that bis-(2-hydroxynaphthaldehyde)-1,2-phenylenediamine is applied as capping agent in presence of tepa for the synthesis of nanostructured $Nd(OH)_3$ and Nd_2O_3 through a facile hydrothermal process. Applying of the new compounds with specific architecture may be advantageous and provide a novel approach for size

and shape-controlled synthesizing of the nanostructured materials. This way is facile, convenient and cost-effective; and opens an effective approach to the production of other hydroxide and oxide materials. We have investigated the effects of precipitator type, reaction time and applying Schiff base ligand as novel capping agent on the grain size and shape of the final products.

2 Experimental

2.1 Materials and characterization

Liquor ammonia solution containing 25% ammonia, methanol, neodymium nitrate ($Nd(NO_3)_3{\cdot}6H_2O$), ethylenediamine (en), 1,2-phenylenediamine ($C_6H_4(NH_2)_2$), tetraethylenepentamine (tepa), 2-hydroxynaphthaldehyde ($C_{11}H_8O_2$) and triethylenetetramine (Trien), with analytical grade were bought from Merck and were applied without additional purification. GC-2550TG (Teif Gostar Faraz Company, Iran) were used for all chemical analyses. Powder X-ray diffraction (XRD) patterns of as-formed nanostructured $Nd(OH)_3$ and Nd_2O_3 were collected from a Philips diffractometer applying X'PertPro and the monochromatized Cu Ka radiation (l = 1.54 Å). The UV–vis diffuse reflectance spectrum of the as-prepared nanostructured Nd_2O_3 was obtained on a UV–vis spectrophotometer (Shimadzu, UV-2550, Japan). Morphological features of the $Nd(OH)_3$ and Nd_2O_3 products were evaluated by a Tescan mira3 field emission scanning electron microscope (FESEM). The energy dispersive spectrometry (EDS) analysis was evaluated by Tescan mira3 microscope. Fourier transform infrared spectra of the as-formed samples were obtained applying KBr pellets on an FT-IR spectrometer (Magna-IR, 550 Nicolet) in the 400–4000 cm^{-1} range. TEM micrographs of as-produced nanostructured Nd_2O_3 were obtained on a JEM-2100 with an accelerating voltage of 200 kV equipped with a high resolution CCD Camera. Thermogravimetric-differential thermal test (TG-DTA) was performed by a thermal gravimetric analysis instrument (Shimadzu TGA-50H) with a flow rate of 20.0 ml min^{-1} and a heating rate of 10 °C min^{-1}.

2.2 Synthesis of bis-(2-hydroxynaphthaldehyde)-1,2 -phenylenediamine capping agent

For preparing the capping agent, 0.08 mol of 2-hydroxynaphthaldehyde dissolved in methanol (35 ml) was added drop-wise to the 1,2-phenylenediamine solution (0.04 mol in 50 ml of methanol). The resultant precipitate of the capping agent was produced after refluxing the mixture for 180 min, separating by filtering, washing and air-drying. The capping agent was ultimately recrystallized from methanol.

2.3 Synthesis of the nanostructured $Nd(OH)_3$ and Nd_2O_3 samples

Nanostructured $Nd(OH)_3$ and Nd_2O_3 samples were synthesized through a novel simple hydrothermal way. For synthesizing nanostructured $Nd(OH)_3$, in a typical procedure, 0.08 g of neodymium nitrate was dissolved in 20 ml distilled water. The pH of the resultant neodymium nitrate solution was adjusted to 12 by drop-wise adding tetraethylenepentamine solution under constant stirring. After 10 min stirring the obtained solution was transferred in a Teflon-lined stainless steel autoclave and heated at 140 °C for 14 h. The resulting precipitate was filtered, washed out with distilled water and ethanol for three times, air-dried (sample no. 4). In order to evaluate the effect of the capping agent, a stoichiometric quantity of the capping agent was dissolved in 4 ml methanol and added to neodymium nitrate solution before adding tetraethylenepentamine solution. In addition to, the effect of the precipitator type, reaction time and applying bis-(2-hydroxynaphthaldehyde)-1,2-phenylenediamine as new capping agent on the grain size and shape of the products were examined (Table 1). For preparing the nanostructured Nd_2O_3 sample, the as-produced nanostructured $Nd(OH)_3$ (sample no. 8) was calcined at 700 °C for 4 h. Schematic diagram of the preparation of the nanostructured $Nd(OH)_3$ and Nd_2O_3 samples (sample nos. 11 and 12) is illustrated in Fig. 1.

2.4 Photocatalytic tests

The photocatalytic performance of the as-produced Nd_2O_3 samples with various particle sizes and shapes (sample nos. 5, 8 and 12) was evaluated by employing eriochrome black T dye solution. The solution containing 2 mg of the

Table 1 The preparation conditions of the neodymium hydroxide and neodymium oxide nanostructures

Sample no.	Calcination at 700 °C	Reaction duration (h)	Capping agent	Precipitator	Figure of SEM images
1	–	14	–	NH_3	6a
2	–	14	–	en	6b
3	–	14	–	Trien	6c
4	–	14	–	Tepa	6d
5	+	14	–	NH_3	7a
6	+	14	–	en	7b
7	+	14	–	Trien	7c
8	+	14	–	Tepa	7d
9	–	10	–	Tepa	8a
10	–	18	–	Tepa	8b
11	–	14	+	Tepa	9a
12	+	14	+	Tepa	9b

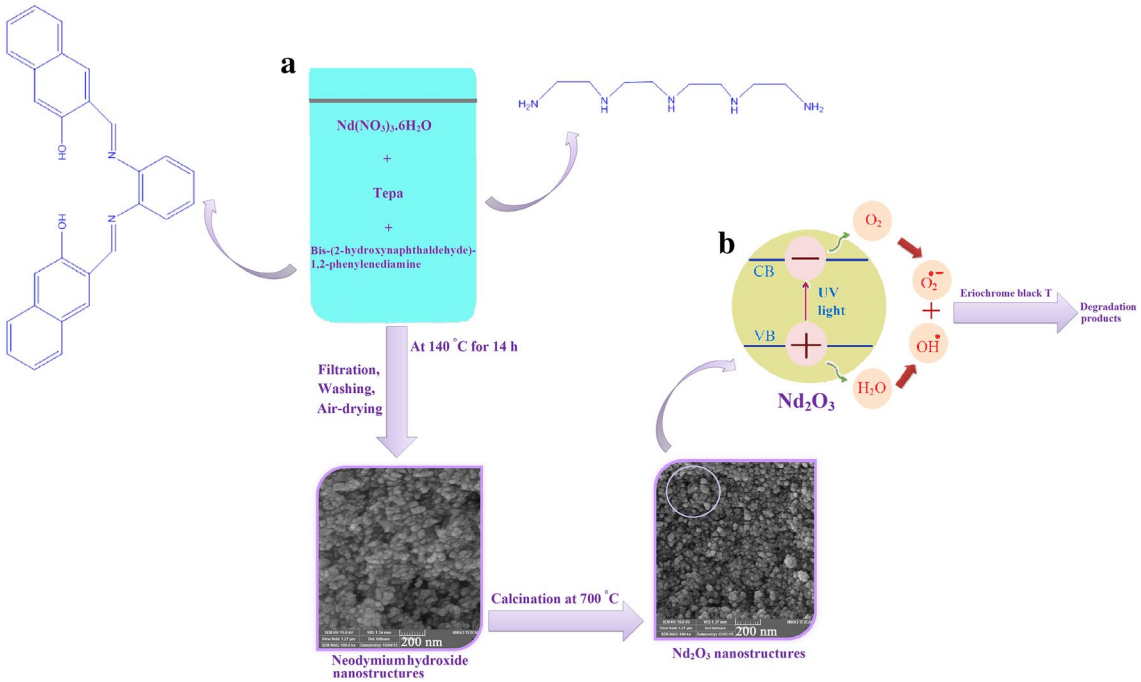

Fig. 1 Schematic diagram of the preparation of the nanostructured $Nd(OH)_3$ and Nd_2O_3 samples (**a**) and reaction mechanism of eriochrome black T photodegradation over nanostructured Nd_2O_3 under UV light illumination (**b**)

eriochrome black T and 80 mg of the as-produced Nd_2O_3 sample in the quartz reactor was utilized to carry out the photocatalytic test. After aerating for 1/2 h, the resulting mixture was subjected to the irradiation of the UV light from the 400 W mercury lamps. The value of eriochrome black T dye was checked on the basis of its UV–visible absorption quantity.

3 Results and discussion

For determining the preparation of the capping agent, nanostructured $Nd(OH)_3$ (sample no. 11) and Nd_2O_3 (sample no. 12) samples, FT-IR analysis was carried out. The infrared spectra of the capping agent, as-synthesized nanostructured $Nd(OH)_3$ (sample no. 11) and Nd_2O_3 (sample no. 12) samples are depicted in Fig. 2a–c, respectively. In the FT-IR spectrum of the capping agent (Fig. 2a), the peaks appear at 1616 and 1322 cm^{-1} are corresponding to the ν(C=N) and ν(Ar–O), respectively, which confirms the preparation of the capping agent [24]. In the FT-IR spectrum of nanostructured $Nd(OH)_3$ (sample no. 11) sample, O–H stretching vibration of $Nd(OH)_3$ and the O–H bending vibration of Nd–O–H appear at 3606 and 676 cm^{-1} (Fig. 2b). In Fig. 2b, the (C–H) bending vibration band at 1384 cm^{-1} exhibits the presence of tetraethylenepentamine. Besides the band appears at 858 cm^{-1} in Fig. 2b is attributable to the carbonate group [25]. It seems that the neodymium hydroxide synthesized at the hydrothermal procedure has high affinity to the atmospheric carbon dioxide, therefore converting to the hydroxy-carbonate phase during washing stages and very small quantity of the hydroxy-carbonate phase forms. In the FT-IR spectrum of the nanostructured Nd_2O_3 (sample no. 12) sample, the absorption band appears at 3425 cm^{-1} is attributable to the ν(OH) stretching vibration of physisorbed water molecules [25]. The characteristic peak of the Nd_2O_3 appears at 500 cm^{-1} [26] (Fig. 2c).

Thermal gravimetric test (TGA) was performed to evaluate the thermal stability of the as-produced nanostructured neodymium hydroxide (sample no. 11). The TGA curve of the as-synthesized nanostructured neodymium hydroxide is depicted in Fig. 3. One mass loss step occurred in the 25–215 °C (showing 1.72% mass loss) are possibly attributable to surface moisture evaporating. Other mass loss step occurred in the 215–700 °C (illustrating 14.96% mass loss) can be related to the chemical conversion: $2Nd(OH)_3 \rightarrow Nd_2O_3 + 3H_2O$ [27] and the preparation of neodymium oxide.

To evaluate the chemical composition of the as-prepared nanostructured neodymium oxide (sample no. 12), EDS test was performed. The EDS spectrum of the sample no. 12 is depicted in Fig. 4. The EDS pattern illustrates that the only existing elements in this synthesized sample are Nd and O.

To characterize the crystal structure of the as-produced nanostructured neodymium hydroxide (sample no. 11) and neodymium oxide (sample no. 12) samples, XRD patterns

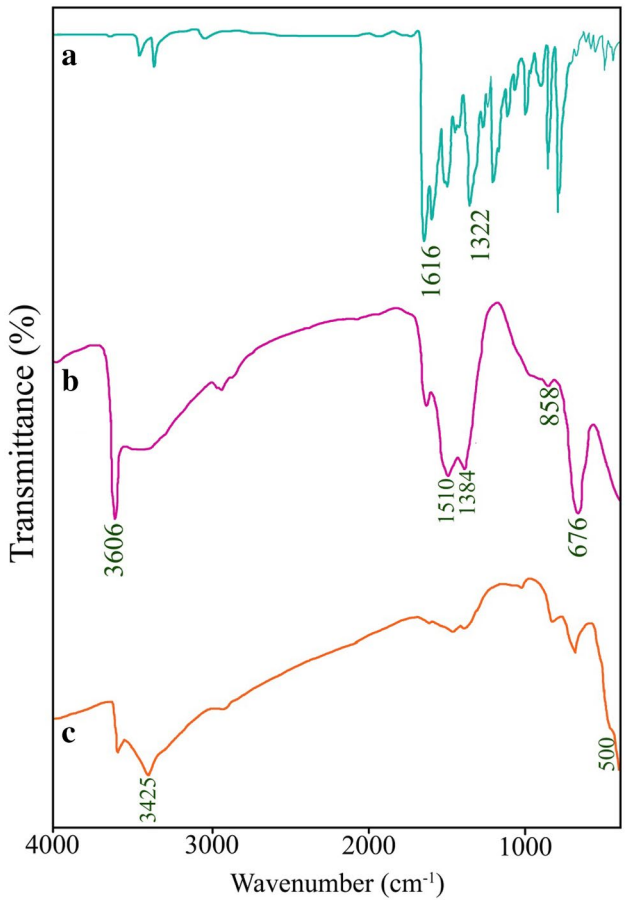

Fig. 2 FT-IR spectra of the capping agent (*a*), as-prepared nanostructured $Nd(OH)_3$ (sample no. 11) (*b*) and Nd_2O_3 (sample no. 12) (*c*) products

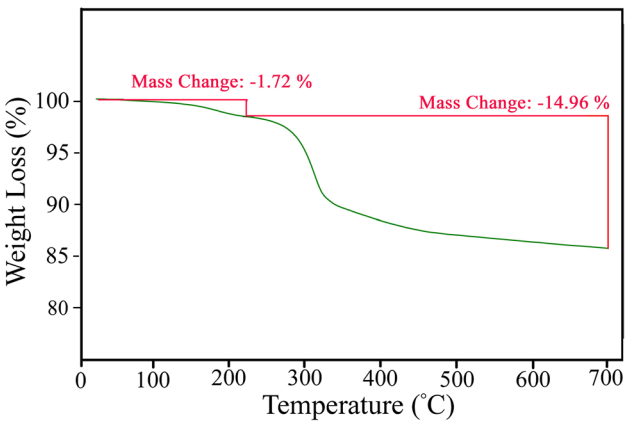

Fig. 3 TGA of the as-produced nanostructured $Nd(OH)_3$ (sample no. 11)

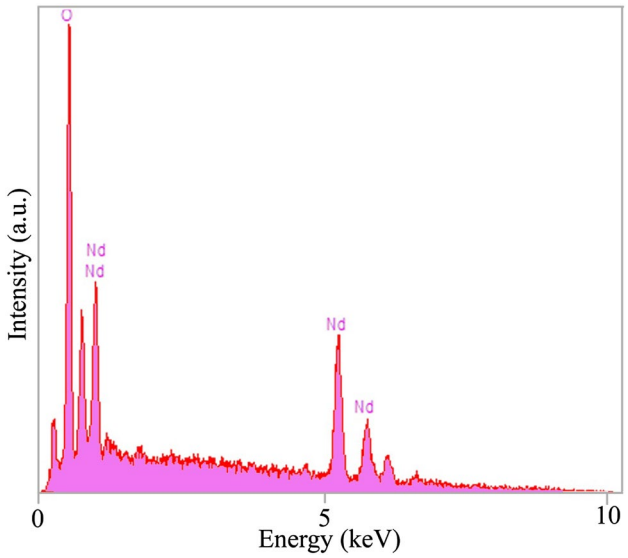

Fig. 4 EDS pattern of the as-obtained nanostructured Nd_2O_3 (sample no. 12)

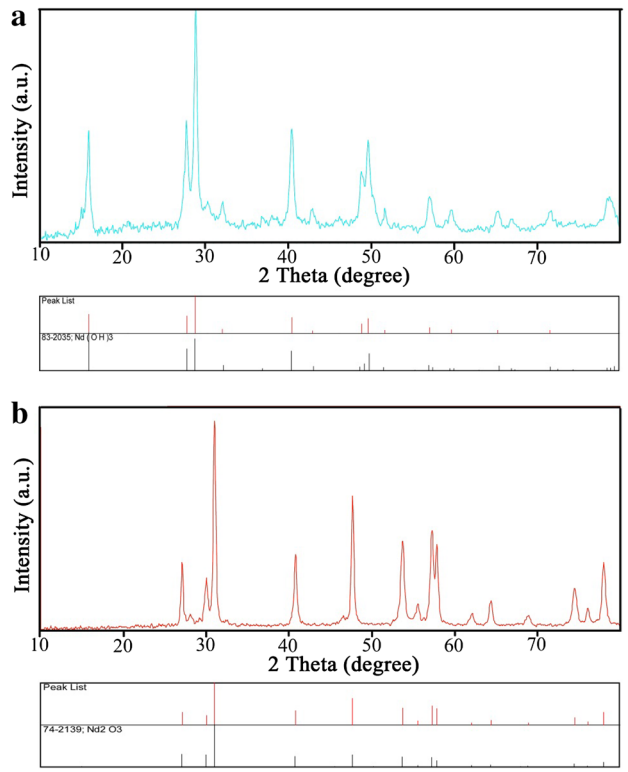

Fig. 5 XRD patterns of the as-synthesized nanostructured $Nd(OH)_3$ (sample no. 11) (**a**) and Nd_2O_3 (sample no. 12) (**b**) products

were taken and depicted in Fig. 5a, b. As observed in the XRD pattern of the nanostructured neodymium hydroxide (sample no. 11), all the diffraction peaks are well-matched to pure hexagonal $Nd(OH)_3$ with P63/m space group (JCPDS 83-2035). All the diffraction bands depicted in Fig. 5b can be readily indexed to pure hexagonal Nd_2O_3 (JCPDS card 74-2139). The average crystallite size of the as-produced

nanostructured neodymium oxide (sample no. 12) sample calculated by applying the Scherrer equation [22] is 26 nm. Thus, the XRD, EDS and FT-IR results reveal the high purity of the as-produced nanostructured neodymium oxide (sample no. 12) sample in this investigation.

As described before, in this investigation nanostructured neodymium hydroxide were synthesized through a novel facile hydrothermal procedure with neodymium nitrate and tetraethylenepentamine (tepa) as starting materials in presence of bis-(2-hydroxynaphthaldehyde)-1,2-phenylenediamine as novel capping agent. Bis-(2-hydroxynaphthaldehyde)-1,2-phenylenediamine with high steric hindrance influence was employed as capping agent in presence of tepa to control the shape and grain size and produce nanostructured neodymium hydroxide for the first time. Pure hexagonal nanostructured neodymium oxide was obtained by thermal conversion of nanostructured neodymium hydroxide in air at 700 °C for 4 h. Preparation of neodymium hydroxide at 140 °C for 14 h has been selected as a basic reaction in this investigation and the effects of the precipitator type, reaction time and applying Schiff base ligand as novel capping agent on the shape and particle size of the products have been examined by SEM technique. The precipitator type influence on the grain size and shape of the neodymium hydroxide and neodymium oxide were examined. For this goal, four reactions were carried out by applying the ammonia (sample no. 1), ethylenediamine (sample no. 2), triethylenetetramine (sample no. 3) and tetraethylenepentamine (sample no. 4). The SEM images reveal that the irregular micro/nanostructures (Fig. 6a), irregular spherical nanobundles (Fig. 6b), irregular nanorods/not uniform spherical nanoparticles (Fig. 6c) and relatively uniform nanorods (Fig. 6d) are prepared by applying the ammonia, ethylenediamine, triethylenetetramine and tetraethylenepentamine, respectively (Fig. 6a–d). It seems that when the precipitator type changes, the grain size decreases with enhancing steric hindrance influence. It seems that when the steric hindrance influence enhances, the aggregation between

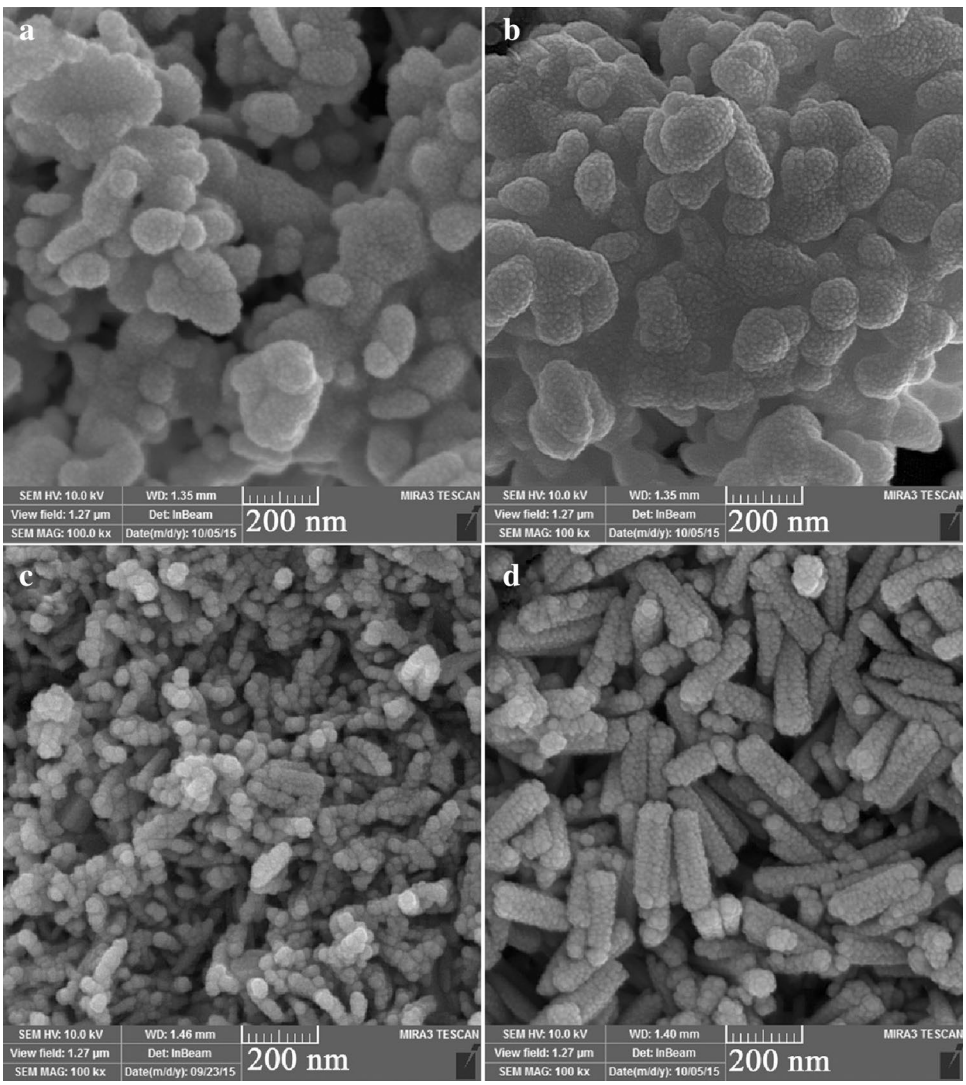

Fig. 6 SEM images of the neodymium hydroxide samples prepared by applying the ammonia (**a**), ethylenediamine (**b**), triethylenetetramine (**c**) and tetraethylenepentamine (**d**)

formed neodymium hydroxide nanoparticles decreases and nucleation to be taken place rather than the particle growth. By changing the precipitator type from ammonia to tetraethylenepentamine, the applied precipitator types with different steric hindrance influence can play a capping agent role and can provide the various reaction interfaces for formed neodymium hydroxide nanoparticles and induce the neodymium hydroxide nanoparticles to assemble in the definite directions, and thus micro/nanostructures, spherical nanobundles, spherical nanoparticles and nanorods were synthesized, respectively. The corresponding neodymium oxides were obtained by calcination at 700 °C for 4 h (Fig. 7a–d). The SEM images illustrate that the high agglomerated particles/irregular micro structures (Fig. 7a), irregular agglomerated spherical nanobundles (Fig. 7b), not uniform nanobundles (Fig. 7c) and relatively uniform nanorods (Fig. 7d) were synthesized by applying the ammonia (sample no. 5), ethylenediamine (sample no. 6), triethylenetetramine (sample no. 7) and tetraethylenepentamine (sample no. 8). Hence, the precipitator type has a considerable impact on the shape and grain size control of the neodymium hydroxide and neodymium oxide. Results of SEM studies reveal that tetraethylenepentamine is the most favorable precipitator in our hydrothermal reaction conditions (Figs. 6d, 7d), thus other hydrothermal reactions were carried out by applying the tetraethylenepentamine.

In continuation, the reaction duration influence on the shape and grain size of the neodymium hydroxide was investigated. The reaction duration was altered to 10 and 18 h and the neodymium hydroxide samples were prepared at 140 °C (sample nos. 9 and 10). SEM images of the neodymium hydroxide samples produced at 10 and 18 h were taken and depicted in Fig. 8a, b. The sample no. 9 prepared at 10 h reveals the not uniform spherical nanoparticles. The SEM image in Fig. 8b obviously reveals that irregular nanobundles were obtained. It can be seen that the morphology changes from relatively uniform nanorods to not uniform spherical nanoparticles (sample no. 9) and the irregular nanobundles

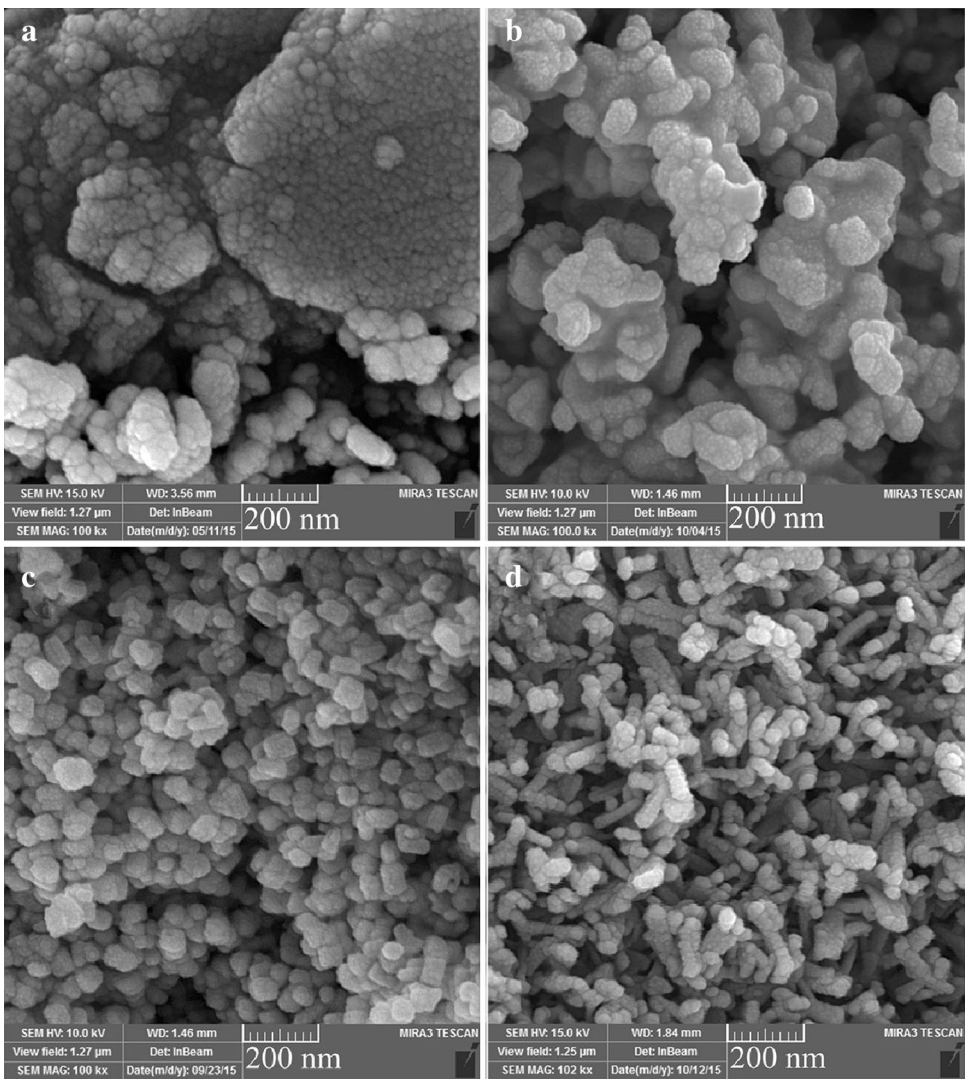

Fig. 7 SEM images of the neodymium oxide products prepared by employing the ammonia (**a**), ethylenediamine (**b**), triethylenetetramine (**c**) and tetraethylenepentamine (**d**)

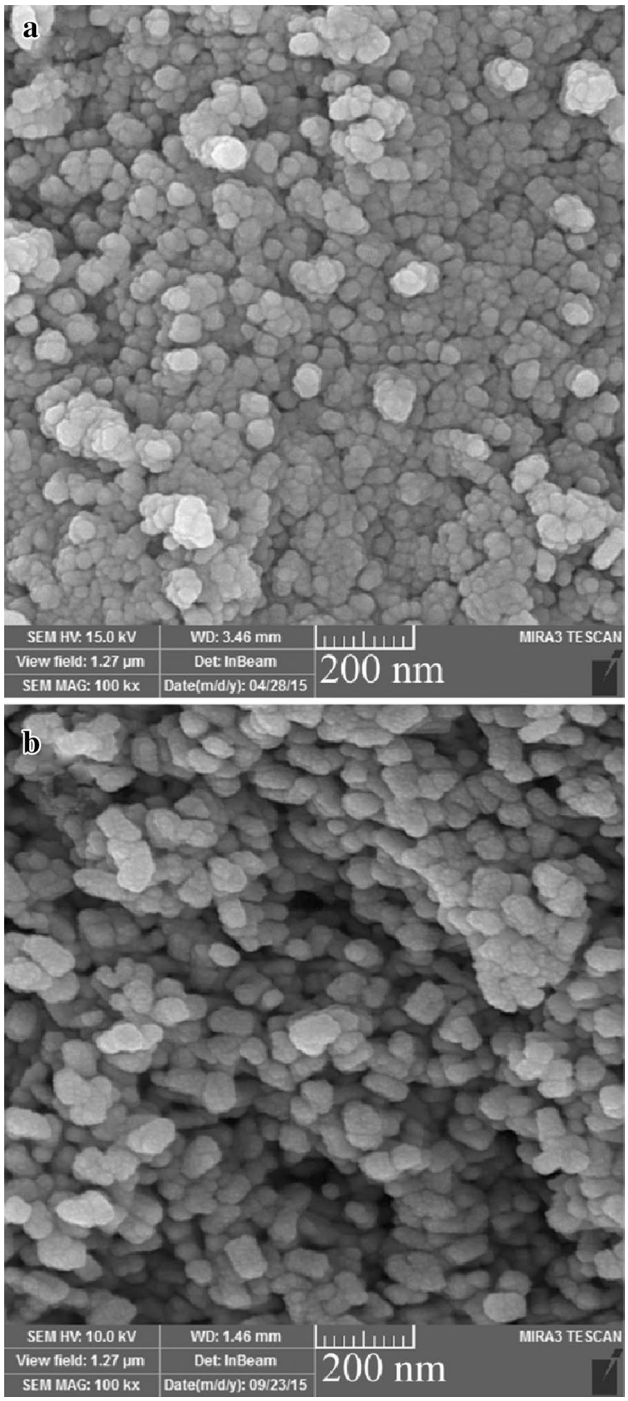

Fig. 8 SEM images of the neodymium hydroxide samples synthesized at 140 °C for (**a**) 10 and (**b**) 18 h

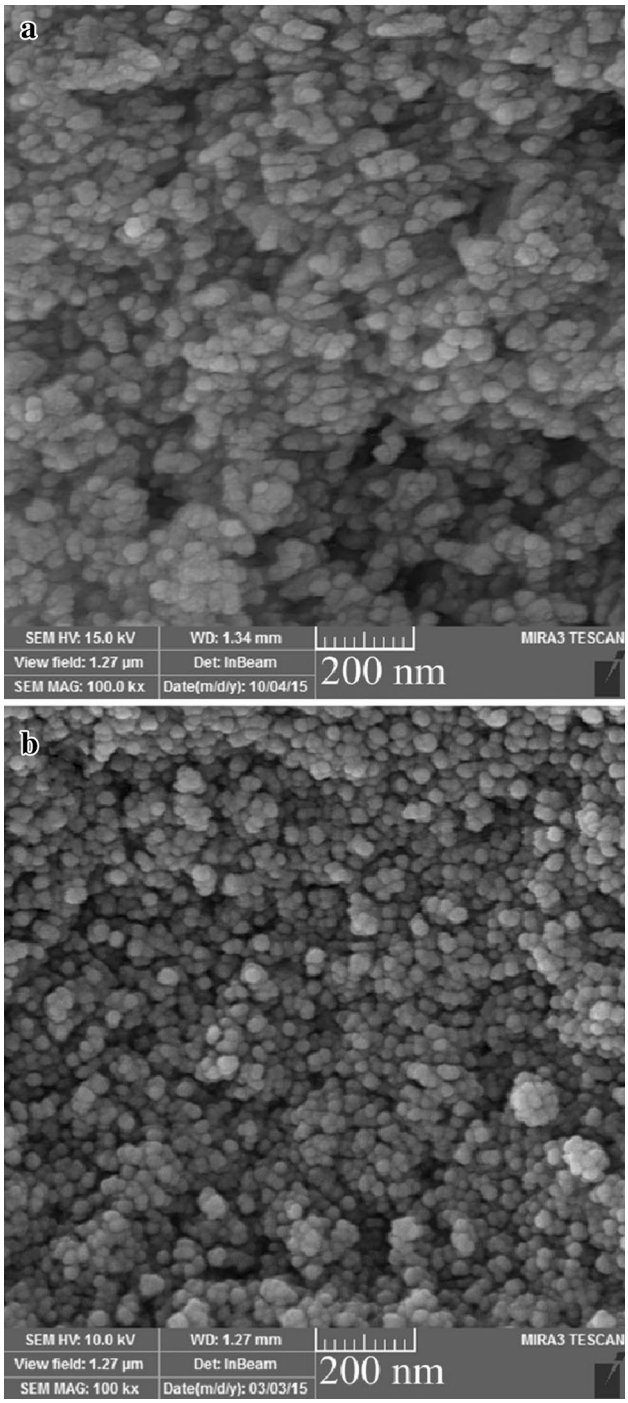

Fig. 9 SEM images of the neodymium hydroxide sample prepared by applying the new capping agent in presence of tepa (**a**) and SEM image of the as-produced nanostructured Nd_2O_3 (**b**)

(sample no. 10) by changing the reaction duration from 14 to 10 and 18 h. This happened change in morphology can be related to the Ostwald ripening process.

Moreover, the influence of the bis-(2-hydroxynaphthaldehyde)-1,2-phenylenediamine capping agent on the particle size and shape the neodymium hydroxide and neodymium oxide was examined. SEM image of the neodymium hydroxide (sample no. 11) and neodymium oxide (sample no. 12) synthesized by employing the novel capping agent was taken and indicated in Fig. 9a, b. By employing the capping agent, uniform spherical neodymium hydroxide nanoparticles and very homogenous neodymium

oxide are obtained (Fig. 9a, b). This new capping agent with high steric hindrance influence can limit the grain size of the neodymium hydroxide nanoparticles via protecting them from further aggregation. It is apparent that employing this new capping agent results in uniform spherical neodymium hydroxide nanoparticles as well as very homogenous neodymium oxide nanoparticles preparation (Fig. 9a, b). Thus, an excellence of the employing this new capping agent in presence of tetraethylenepentamine is that it causes to prepare nanostructured neodymium hydroxide and neodymium oxide.

Based on the SEM results, it can be deduced that employing bis-(2-hydroxynaphthaldehyde)-1,2-phenylenediamine as new capping agent in presence of tetraethylenepentamine and reaction time = 14 h are the optimum condition for uniform spherical neodymium hydroxide nanoparticles as well as very homogenous neodymium oxide nanoparticles preparation with small particle size (Fig. 9a, b).

To elucidate the detailed shape and size of the as-produced neodymium oxide sample (sample no. 8), the typical TEM images were taken. Figure 10a, b reveals TEM images of neodymium oxide product is synthesized by calcining nanostructured neodymium hydroxide (sample no. 4), illustrating nanorods with lengths and diameters of 22–40 and 60–120 nm, respectively (Fig. 10).

UV–vis diffuse reflectance spectrum was taken to examine the optical characteristics and band gap (Eg) of as-produced neodymium oxide product (sample no. 12). Figure 11a depicts the UV–vis diffuse reflectance spectrum of the neodymium oxide product. The absorption peak appears at 367 nm in Fig. 11a. The band gap may be calculated based on the absorption spectrum by utilizing Tauc's relationship [3]. The Eg of the neodymium oxide product (sample no. 12) may be determined by extrapolating $(\alpha h\nu)^2$ against $h\nu$ at $(\alpha h\nu)^2 = 0$ [3, 22] (Fig. 11b). The energy gap quantity of the neodymium oxide product (sample no. 12) calculated to be 3.32 eV. From the determined Eg quantity, the as-synthesized neodymium oxide product may be utilized as the photocatalyst material.

To illustrate the photocatalytic performance of as-produced Nd_2O_3 samples with various particle sizes and shapes (sample nos. 5, 8 and 12) for the degradation contaminants, the photodegradation of eriochrome black T (anionic dye) tests were carried out under UV light irradiation. High agglomerated particles/irregular micro structures (sample no. 5), relatively uniform nanorods (sample no. 8) and very homogenous spherical neodymium oxide nanoparticles (sample no. 12) produced by applying ammonia and tetraethylenepentamine without and with novel capping agent have been employed for degradation of eriochrome black T and their photocatalytic performance have been compared on 100 min. The result of the photocatalytic experiments are depicted in Figs. 12, 13. No anionic dye was almost broken down after 100 min in absence

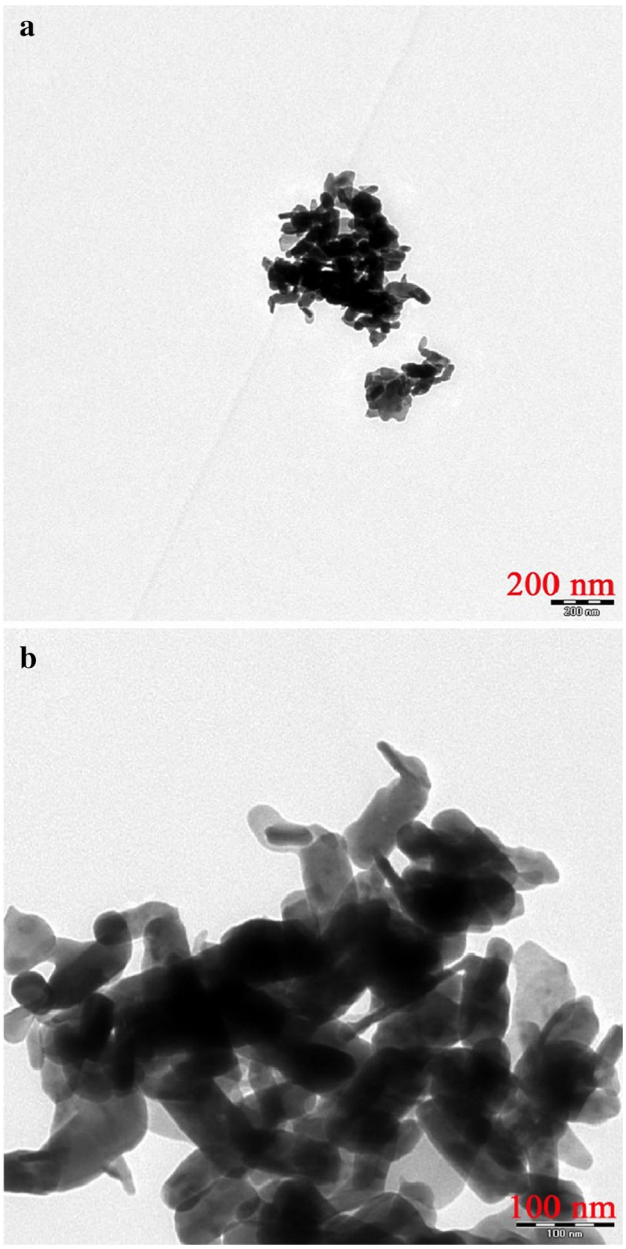

Fig. 10 TEM images of the as-produced nanostructured Nd_2O_3 (sample no. 8)

of the UV light or as-synthesized neodymium oxide products (sample nos. 5, 8 and 12). This observed result indicated that the share of self-degradation was insignificant. The probable mechanism of the photodegradation of anionic dye may be assumed as [28, 29]:

$$\text{Nanostructured } Nd_2O_3 + h\nu \rightarrow \text{Nanostructured } Nd_2O_3{}^{*} + e^{-} + h^{+}$$

$$h^{+} + e^{-} \rightarrow \text{heat}$$

$$h^{+} + H_2O \rightarrow OH^{\cdot} + H^{+}$$

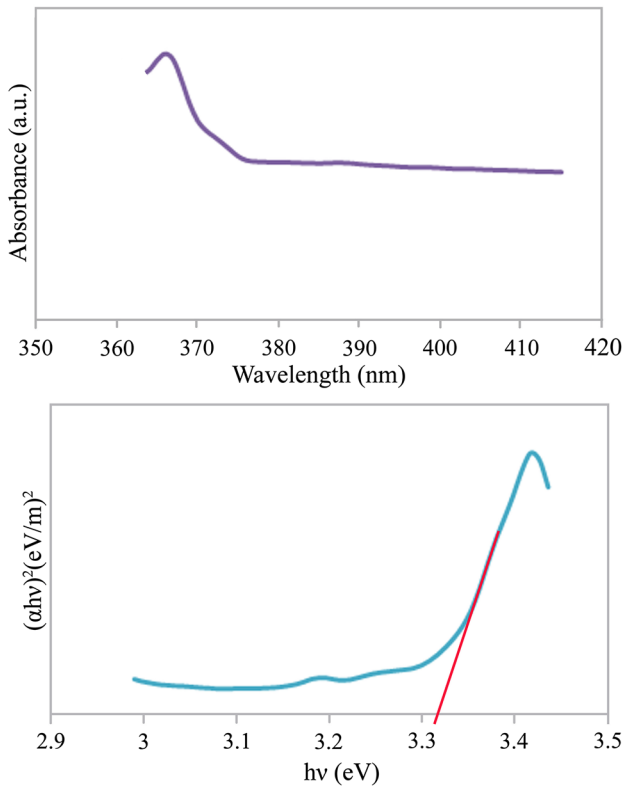

Fig. 11 UV–vis diffuse reflectance spectrum (**a**) and plot to determine the band gap (**b**) of the as-produced nanostructured Nd_2O_3 (sample no. 12)

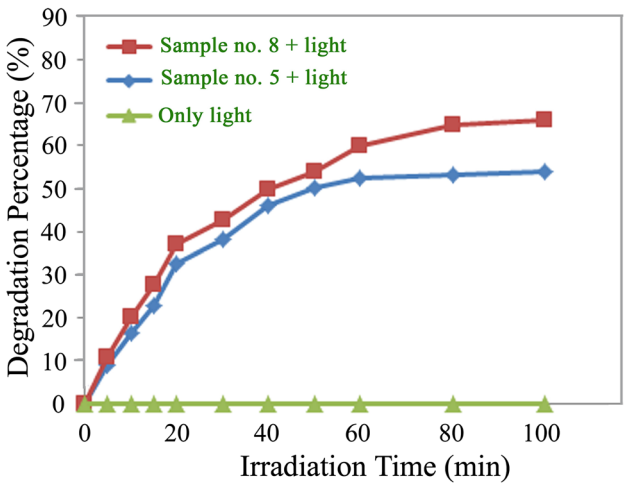

Fig. 12 Photocatalytic anionic dye (eriochrome black T) degradation of the sample nos. 5 and 8

$$h^+ + OH^- \rightarrow OH^{\cdot}$$

$$e^- + O_2 \rightarrow O_2^{-\cdot}$$

$$O_2^{-\cdot} + HO_2^{\cdot} + H^+ \rightarrow H_2O_2 + O_2$$

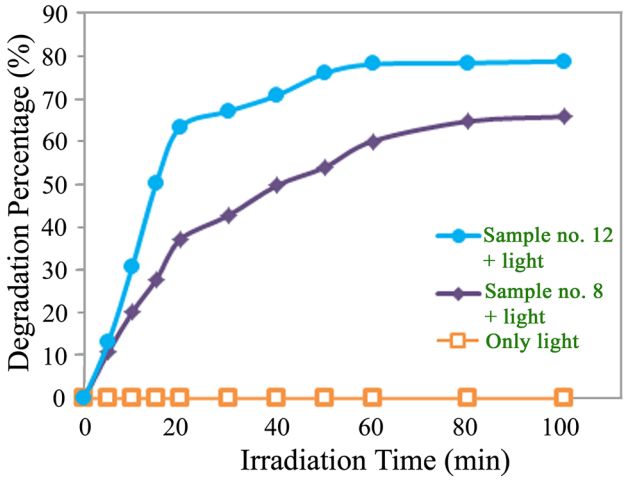

Fig. 13 Photocatalytic anionic dye (eriochrome black T) degradation of the sample nos. 8 and 12

$$O_2^{-\cdot} + \text{Anionic dye} \rightarrow \text{Degradation products} + OO^{\cdot}$$

The percentage of anionic dye photodegradation was obtained as follows:

$$D.P.\ (t) = \frac{A_0 - A_t}{A_0} \times 100 \quad (1)$$

where A_0 and A_t are the absorbance value of anionic dye solution at before and after photodegradation by utilizing a UV–vis spectrometer, respectively. The anionic dye photodegradation was about 54% by (sample no. 5), 66% by (sample no. 8) and 79% by (sample no. 12) after 100 min irradiation of UV light and the as-formed neodymium oxide product (sample no. 12) illustrated very fine photocatalytic performance. By considering the photocatalytic results and shape and particle size of neodymium oxide products (Figs. 7a, d, 9b), it can be seen that photocatalytic efficiency of the homogenous spherical neodymium oxide nanoparticles (sample no. 12) is higher than that of the high agglomerated particles/irregular micro structures (sample no. 5) and relatively uniform nanorods (sample no. 8) due to their greater surface area. The neodymium oxide nanoparticles (sample no. 12) with smallest grain size owing to large surface area can reveal the best photocatalytic performance. Hence shape and particle size of neodymium oxide is a substantial parameter on destruction of water pollutant. The heterogeneous photocatalytic processes have diffusion, adsorption and reaction stages. It is well known that the appropriate distribution of the pore has considerable and effective impact on the diffusion of the reactants and products, and hence influences on the photocatalytic performance. It seems that the enhanced photocatalytic performance of the as-formed neodymium oxide product (sample no. 12) can be corresponding to appropriate and favorable distribution of the

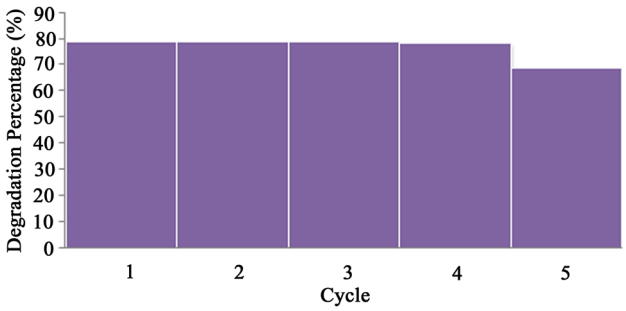

Fig. 14 Recycling tests of the as-formed nanostructured Nd_2O_3 (sample no. 12) for destruction of eriochrome black T under ultraviolet illumination

pore, great hydroxyl quantity and very fine separation rate of charge carriers [30] (Fig. 1). In addition, repeated destruction reactions have been done to elucidate the stability of the as-formed neodymium oxide (sample no. 12). It can be seen that as-formed neodymium oxide (sample no. 12) did not reveal any remarkable loss of performance after 4 sequential reaction cycles (Fig. 14), presenting superior stability of catalyst. The destruction efficiency has been diminished to 68.9% after 5 cycles.

4 Conclusions

In summary, $Nd(OH)_3$ nanostructures have been successfully prepared from $Nd(NO_3)_3{\cdot}6H_2O$ and tetraethylenepentamine (tepa) as starting materials in presence of bis-(2-hydroxynaphthaldehyde)-1,2-phenylenediamine as novel capping agent, using a new simple morphology-controlled hydrothermal approach. Pure hexagonal Nd_2O_3 nanostructures were synthesized by thermal conversion of nanostructured $Nd(OH)_3$ in air at 700 °C for 4 h. To the best of our knowledge, it is the first time that bis-(2-hydroxynaphthaldehyde)-1,2-phenylenediamine is employed as capping agent in presence of tepa to produce nanostructured $Nd(OH)_3$ and Nd_2O_3. By changing the precipitator type and reaction time as well as applying Schiff base ligand as novel capping agent, we could obtain $Nd(OH)_3$ and Nd_2O_3 nanostructures with the different shapes and particle sizes. This process is proved to be a new, low cost, simple and efficient approach. In addition, the photocatalytic performance of as-produced Nd_2O_3 samples with various particle sizes and shapes was investigated. The as-formed neodymium oxide can be applied as considerable and desirable materaial for photocatalytic usages under irradiation of UV light such as deletion of eriochrome black T dye, since this dye photooxidation percentage was found to be 79 within 100 min.

Acknowledgements Authors are grateful to the council of Iran National Science Foundation (INSF) and University of Kashan for supporting this work by Grant No. (159271/83990).

References

1. F. Beshkar, S. Zinatloo-Ajabshir, M. Salavati-Niasari, Simple morphology-controlled fabrication of nickel chromite nanostructures via a novel route. Chem. Eng. J. **279**, 605–614 (2015)
2. S. Zinatloo-Ajabshir, M. Salavati-Niasari, A. Sonochemical-Assisted, Synthesis of pure nanocrystalline tetragonal zirconium dioxide using tetramethylethylenediamine. Int. J. Appl. Ceram. Technol. **11**, 654–662 (2014)
3. S. Moshtaghi, S. Zinatloo-Ajabshir, M. Salavati-Niasari, Nanocrystalline barium stannate: facile morphology-controlled preparation, characterization and investigation of optical and photocatalytic properties. J. Mater. Sci. **27**, 834–842 (2016)
4. M. Cheng, S. Yang, R. Chen, X. Zhu, Q. Liao, Y. Huang, Copper-decorated TiO_2 nanorod thin films in optofluidic planar reactors for efficient photocatalytic reduction of CO_2. Int. J. Hydrogen Energy **42**, 9722–9732 (2017)
5. H. Sun, X. Zhou, H. Zhang, W. Tu, An efficient exfoliation method to obtain graphitic carbon nitride nanosheets with superior visible-light photocatalytic activity. Int. J. Hydrogen Energy **42**, 7930–7937 (2017)
6. M. Masjedi-Arani, M. Salavati-Niasari, Facile precipitation synthesis and electrochemical evaluation of Zn_2SnO_4 nanostructure as a hydrogen storage material. Int. J. Hydrogen Energy **42**(17), 12420–12429 (2017)
7. S. Mandizadeh, M. Sadri, M. Salavati-Niasari, Sol–gel auto combustion synthesis of $BaFe_{18}O_{27}$ nanostructures for adsorptive desulfurization of liquid fuels. Int. J. Hydrogen Energy **42**, 12320–12326 (2017)
8. M. Zawadzki, L. Kpiński, Synthesis and characterization of neodymium oxide nanoparticles. J. Alloys Compd. **380**, 255–259 (2004)
9. F. Delorme, C. Harnois, I. Monot-Laffez, G. Desgardin, Nd_2O_3 doping of top-seeding-melt-texture-growth-processed $YBa_2Cu_3O_{7-\delta}$ ceramics. Physica C **372–376**(Part 2), 1127–1130 (2002)
10. A. Kosola, J. Päiväsaari, M. Putkonen, L. Niinistö, Neodymium oxide and neodymium aluminate thin films by atomic layer deposition. Thin Solid Films **479**, 152–159 (2005)
11. C.R. Michel, A.H. Martínez-Preciado, N.L.L. Contreras, Gas sensing properties of Nd_2O_3 nanostructured microspheres. Sens. Actuators B **184**, 8–14 (2013)
12. T. Liu, Y. Zhang, H. Shao, X. Li, Synthesis and characteristics of Sm_2O_3 and Nd_2O_3 nanoparticles. Langmuir **19**, 7569–7572 (2003)
13. W. Zhu, J. Ma, L. Xu, W. Zhang, Y. Chen, Controlled synthesis of $Nd(OH)_3$ and Nd_2O_3 nanoparticles by microemulsion method. Mater. Chem. Phys. **122**, 362–367 (2010)
14. T. Sreethawong, S. Chavadej, S. Ngamsinlapasathian, S. Yoshikawa, Sol–gel synthesis of mesoporous assembly of Nd_2O_3 nanocrystals with the aid of structure-directing surfactant. Solid State Sci. **10**, 20–25 (2008)
15. S.V. Chavan, P.U.M. Sastry, A.K. Tyagi, Combustion synthesis of nano-crystalline Nd-doped ceria and Nd_2O_3 and their fractal behavior as studied by small angle X-ray scattering. J. Alloys Compd. **456**, 51–56 (2008)
16. L. Kępiński, M. Zawadzki, W. Miśta, Hydrothermal synthesis of precursors of neodymium oxide nanoparticles. Solid State Sci. **6**, 1327–1336 (2004)
17. Q. Liqin, W. Kaituo, W. Xuehang, W. Wenwei, L. Sen, L. Gengming, Nanocrystalline Nd_2O_3: preparation, phase evolution, and

kinetics of thermal decomposition of precursor. Ceram. Int. **40**, 3003–3009 (2014)
18. S. Zinatloo-Ajabshir, M. Salavati-Niasari, Z. Zinatloo-Ajabshir, $Nd_2Zr_2O_7$-Nd_2O_3 nanocomposites: new facile synthesis, characterization and investigation of photocatalytic behaviour. Mater. Lett. **180**, 27–30 (2016)
19. F. Beshkar, S. Zinatloo-Ajabshir, M. Salavati-Niasari, Preparation and characterization of the $CuCr_2O_4$ nanostructures via a new simple route. J. Mater. Sci. **26**, 5043–5051 (2015)
20. S. Zinatloo-Ajabshir, M. Salavati-Niasari, Novel poly(ethyleneglycol)-assisted synthesis of praseodymium oxide nanostructures via a facile precipitation route. Ceram. Int. **41**, 567–575 (2015)
21. S. Mortazavi-Derazkola, S. Zinatloo-Ajabshir, M. Salavati-Niasari, Novel simple solvent-less preparation, characterization and degradation of the cationic dye over holmium oxide ceramic nanostructures. Ceram. Int. **41**, 9593–9601 (2015)
22. S. Zinatloo-Ajabshir, M. Salavati-Niasari, M. Hamadanian, Praseodymium oxide nanostructures: novel solvent-less preparation, characterization and investigation of their optical and photocatalytic properties. RSC Adv. **5**, 33792–33800 (2015)
23. S. Zinatloo-Ajabshir, M. Salavati-Niasari, Preparation of nanocrystalline cubic ZrO_2 with different shapes via a simple precipitation approach. J. Mater. Sci. **27**, 3918–3928 (2016)
24. C.R. Bhattacharjee, P. Goswami, P. Mondal, Synthesis, reactivity, thermal, electrochemical and magnetic studies on iron(III) complexes of tetradentate Schiff base ligands. Inorg. Chim. Acta **387**, 86–92 (2012)
25. S. Zinatloo-Ajabshir, M. Salavati-Niasari, Facile route to synthesize zirconium dioxide (ZrO_2) nanostructures: structural, optical and photocatalytic studies. J. Mol. Liq. **216**, 545–551 (2016)
26. L.M.S. El-Deen, M.S.A. Salhi, M.M. Elkholy, IR and UV spectral studies for rare earths-doped tellurite glasses. J. Alloys Compd. **465**, 333–339 (2008)
27. J.-G. Kang, Y. Jung, B.-K. Min, Y. Sohn, Full characterization of $Eu(OH)_3$ and Eu_2O_3 nanorods. Appl. Surf. Sci. **314**, 158–165 (2014)
28. F. Fang, L. Kong, J. Huang, S. Wu, K. Zhang, X. Wang, B. Sun, Z. Jin, J. Wang, X.-J. Huang, J. Liu, Removal of cobalt ions from aqueous solution by an amination graphene oxide nanocomposite. J. Hazard. Mat. **270**, 1–10 (2014)
29. S. Sakthivel, B. Neppolian, M.V. Shankar, B. Arabindoo, M. Palanichamy, V. Murugesan, Solar photocatalytic degradation of azo dye: comparison of photocatalytic efficiency of ZnO and TiO_2. Sol. Energy Mater. Sol. Cells **77**, 65–82 (2003)
30. J.b. Zhong, J.z. Li, F.m. Feng, Y. Lu, J. Zeng, W. Hu, Z. Tang, Improved photocatalytic performance of SiO_2–TiO_2 prepared with the assistance of SDBS. J. Mol. Catal. A **357**, 101–105 (2012)